

# Improved Dot Diffusion Using Optimized Diffused Weighting and Class Matrix

Jing-Ming Guo, Member, IEEE and Yun-Fu Liu

Department of Electrical Engineering,  
National Taiwan University of Science and Technology  
Taipei, Taiwan

E-mail: [jmguo@seed.net.tw](mailto:jmguo@seed.net.tw), [liuyunfu@ms33.url.com.tw](mailto:liuyunfu@ms33.url.com.tw)

## ABSTRACT

In this work, a high quality halftone image obtained by dot diffusion is proposed to reduce the deficiency gap with the error diffusion. Four kinds of filters with various sizes obtained by Least-Mean-Square (LMS) are also introduced to simulate the human visual system (HVS). These filters are employed in the optimization procedures for class matrix of size  $8 \times 8$ . According to numerous of simulations, an optimized diffused weighting is determined. Many well-known halftone methods, which include direct binary search (DBS), error diffusion, ordered dithering, and previous dot diffusion are also involved for comparisons. As demonstrated in the experiments, the quality of the proposed dot diffusion is close to some error diffusion and is even superior to the well-known Jarvis and Stucki error diffusion or Mese's dot diffusion. Moreover, the dot diffusion inherently has the parallel processing advantage, which provides much higher executing efficiency than DBS or error diffusion.

**Key words:** dot diffusion, error diffusion, direct binary search, ordered dithering, digital halftoning.

## 1. INTRODUCTION

Digital halftoning [1]-[2] is a technique for changing grayscale images into halftone images. These halftone images can resemble the original images when viewing from a distance by lowpass filtering in human visual system (HVS). The technique is used widely in computer printer-outs, printed books, newspapers and magazines, because these printing processes are limited to the black-and-white format (with and without ink). Another major application of digital halftoning is color quantization with a limited color palette. There are several kinds of halftoning methods, which include ordered dithering [1], dot diffusion [3]-[4], error diffusion [5]-[12] and direct binary search (DBS) [13]. Of these, dot diffusion has compromised image quality and processing efficiency.

The ordered dithering is a parallel method, and is generally distinguished into clustered-dot and dispersed-dot halftone screens. The image quality of ordered dithering is inferior to DBS, error diffusion, as well as dot diffusion, since the error induced from the halftoning procedure is retained in each halftone pixel. Conversely, error diffusion does not have the above-mentioned problem, because the error is designed to be compensated by the neighborhood pixels. Hence, the resulting error-diffused halftone has the pleasant-looking blue noise property [14]. However, the error diffusion was born of lacking parallel processing advantage. Hence, the processing efficiency is much inferior to ordered dithering. For the time being, the DBS is the most powerful halftoning when it comes to image quality. However, the time-consuming iteration-based approach makes it difficult to be realized in commercial printing devices.

Dot diffusion inherently has the parallel processing benefit by cooperating with the so-called class matrix. Previous studies related to the dot diffusion have focused on class matrix

optimization by Knuth [3] and Mese [4]. However, the diffused weighting of the previous two works are fixed in integer fashion, which makes the class matrix optimization itself problematic. In this work two issues: diffused weighting and the size of the diffused area are determined to create better halftone quality which is also able to approximate the error diffusion halftone while maintaining the parallel processing characteristic.

## 2. OVERVIEW OF DOT DIFFUSION

Suppose the original image of size  $P \times Q$  is divided into non-overlapped blocks of size  $M \times N$ . An important media called class matrix, which is of the same size as a divided block, is employed to determine the processing order in a block. The flow chart of dot diffusion is quite similar to error diffusion as shown in Fig. 1. Here we define 255 as a white pixel and 0 as a black pixel. The variable  $x_{i,j}$  denotes the current input value and  $x'_{i,j}$  is the diffused error accumulated from the neighboring processed pixels. The variable  $b_{i,j}$  represents binary output at position  $(i,j)$  and  $v_{i,j}$  is the modified gray output. The variable  $e_{i,j}$  denotes the difference between the modified gray output  $v_{i,j}$  and binary output  $b_{i,j}$ , and the relationships of  $b_{i,j}$ ,  $v_{i,j}$  and  $e_{i,j}$  are organized as below.

$$v_{i,j} = x_{i,j} + x'_{i,j}, \text{ where } x'_{i,j} = \sum_{m=0}^2 \sum_{n=0}^2 \frac{e_{i+m,j+n} \times h_{m,n}}{w}, \quad (1)$$

$$e_{i,j} = v_{i,j} - b_{i,j}, \text{ where } b_{i,j} = \begin{cases} 0, & \text{if } v_{i,j} < 128 \\ 255, & \text{if } v_{i,j} \geq 128 \end{cases}, \quad (2)$$

where the variable  $h_{m,n}$  is the diffused weighting, and the one appears in Knuth's and Mese's methods is shown in Fig. 2. The variable  $x$  denotes the current processing pixel, and the integers in the eight-connected neighborhood are diffused proportions. Since the neighbors in vertical and horizontal orientations are closer to the center, hence the weightings are larger than diagonal orientations. Note that, the error can only diffuse to neighbor pixels that are not binarized yet, which associates to the members in the class matrix with higher value. The variable  $w = \sum_{m=0}^2 \sum_{n=0}^2 h_{m,n}$  is the summation of the diffused weights corresponding to those unprocessed pixels.

As expected by the readers, the processing orders within the class matrix have great influence to the reconstructed image quality. Knuth's optimization approach tries to reduce the number of baron (pixel with no higher pixel value surrounded) and near-baron (pixel with only one higher pixel value surrounded) in the class matrix. The concept is straight forward since the baron results in non-diffusible quantized error, and the near-baron only allows quantized error diffuses in one way. However, the Knuth's approach does not take the human visual system (HVS) into consideration. For this, Mese's method adopts the HVS in [4] to determine an optimized class matrix. During his optimization, the single tone 16 is employed to develop the final class matrix as shown in Table I.

Although the Mese's class matrix provides excellent reconstructed halftones as will be shown in Section 4, we believe that there are still some rooms left for improving. For instance, the optimization of the diffused weighting and the diffused area, these will be carefully manipulated in the next section. Another problem in the optimization process of Mese approach solely single tone of value 16 is utilized in the class matrix training, which causes the reconstructed class matrix difficult to render image regions with different tones.

### 3. IMPROVED DOT DIFFUSION USING OPTIMIZED DIFFUSED WEIGHTING AND CLASS MATRIX

As revealed in the last paragraph of Section 2, two parameters of dot diffusion play important roles in the class matrix optimization: diffused weighting and diffused area. In this following, some filters of different sizes trained by the Least-Mean-Square (LMS) are taken as diffused weightings with alternative diffused areas. The LMS-trained filters are further employed to produce the corresponding optimized class matrices. The details will be elaborated in the following subsections. It is an intuition that as the size of class matrix growing, the benefit of parallel processing decreases as well. In order to preserve the important parallel processing advantage, we try to develop an optimized class matrix of size  $8 \times 8$  throughout this work.

#### 3.1 LMS-trained filters and performance evaluation

The performance evaluation employed in this work is defined as below. For an image of size  $P \times Q$ , the quality of a halftone image is defined as

$$PSNR = 10 \log_{10} \frac{P \times Q \times 255^2}{\sum_{i=1}^P \sum_{j=1}^Q [x_{i,j} - \sum_{m,n \in R} w_{m,n} b_{i+m,j+n}]^2}, \quad (3)$$

where  $x_{i,j}$  is the original grayscale image,  $b_{i,j}$  is the corresponding halftone image,  $w_{m,n}$  is the LMS-trained coefficient at position  $(m,n)$  and  $R$  is the support region of the LMS-trained filter. The procedures of how to obtain a LMS filter will be derived in the next section. Since the LMS filter is used to resemble the HVS, the values inside the filter are taken as the diffused weightings and the size can be taken as the diffused area. In the optimization procedure, the support region  $R$  of four different sizes,  $3 \times 3$ ,  $5 \times 5$ ,  $7 \times 7$  and  $9 \times 9$  are utilized for testing. To measure the quality of halftone image, the size of  $R$  is fixed at  $7 \times 7$ .

The LMS-trained filter  $w$  can be obtained by psychophysical experiments [15]. The other way to derive  $w$  can use a training set of both pairs of grayscale images as Fig. 3 and good halftone result of them. In this work, error diffusion, ordered dithering and direct binary search (DBS) are involved to produce the set. Here we use LMS to produce  $w$  as follows,

$$\hat{x}_{i,j} = \sum_{m,n \in R} w_{m,n} b_{i+m,j+n}, \quad (4)$$

$$e_{i,j}^2 = (x_{i,j} - \hat{x}_{i,j})^2, \quad (5)$$

$$\frac{\partial e_{i,j}^2}{\partial w_{m,n}} = -2e_{i,j} b_{i+m,j+n}, \quad (6)$$

$$\begin{cases} \text{if } w_{m,n} > w_{m,n,opt}, \text{ slope} > 0, w_{m,n} \text{ should be decreased} \\ \text{if } w_{m,n} < w_{m,n,opt}, \text{ slope} < 0, w_{m,n} \text{ should be increased} \end{cases}, \quad (7)$$

$$w_{m,n}^{(k+1)} = w_{m,n}^k + \mu e_{i,j} b_{i+m,j+n}, \quad (8)$$

where  $w_{i,j,opt}$  is the optimum LMS coefficient,  $e_{i,j}^2$  is the MSE between  $x_{i,j}$  and  $\hat{x}_{i,j}$ ,  $\mu$  is the adjusting parameter used to control the convergent speed of the LMS optimum procedure, which is set to be  $10^{-5}$  in our experiments. Some other quality evaluation methods can be found in [16] and [17]. Note that, these filters are all with some basic human visual system characteristics: (1) the diagonal has less sensitivity than the

vertical and horizontal directions and (2) the center portion has the highest sensitivity and it decreases while moving away from the center.

#### 3.2 Class matrix optimization using LMS-trained filter

The LMS-trained filters obtained above are employed for class matrix optimization. Since the LMS filters have the characteristics of HVS, it is reasonable to be taken as the diffused weighting and diffused area. During the class matrix optimization, each member in the class matrix is successively swapped with one of the other 63 members and applied to the eight testing images as shown in Fig. 3. The quality evaluation approach introduced in Section 3.1 is employed to evaluate the two average PSNRs (before swapped and after swapped) of the corresponding dot-diffused halftone images. Only the swapped result with the highest PSNR will be retained as a new class matrix, and then conducts the same above-mentioned procedure until any swapping cannot improve the PSNR anymore. Note that, the Mese's approach only adopts single tone of value 16 for class matrix training, which causes the reconstructed class matrix difficult to perfectly render image regions with different tones. Conversely, in this work eight different nature images are involved in training procedure, which makes the reconstructed class matrix easier adapts to different tones in an image. The steps of the optimization procedure are organized as below.

- Step1. Given an initial class matrix  $C$  (The Mese's class matrix is employed).
- Step2. Four LMS filters of sizes  $3 \times 3$ ,  $5 \times 5$ ,  $7 \times 7$  and  $9 \times 9$  are employed as diffused weighting with different diffused areas in the testing.
- Step3. Suppose the members within class matrix are taken as 1-D sequence. Each member  $C(i)$  in the class matrix is successively swapped with one of the other 63 members  $C(j)$ , where  $i \neq j$ .
- Step4. Evaluating the average PSNR of the dot-diffused halftone images using the class matrix derived from Step 3. The diffused weightings and diffused areas are determined by Step 2. Let LMS filter of size  $7 \times 7$  be the HVS filter indicated in Eq. (3).
- Step5. Suppose the swapped class matrix leads to higher reconstructed image quality, the class matrix is modified as the swapped version. Otherwise, the swapped members within class matrix are returned to the original position.
- Step6. Another member  $C(i)$  in the class matrix is selected, and then performs Step 4 and 5.
- Step7. If any swapping cannot improve the quality of reconstructed dot-diffused image, the optimization procedure is terminated. Otherwise, Step 3 to Step 6 are iteratively performed.

The four final converged class matrix associate to different diffused weightings and diffused areas with the proposed optimization procedure introduced above are shown in Table II, which does not include the class matrices obtained by LMS filter of size  $5 \times 5$ ,  $7 \times 7$  and  $9 \times 9$ , since these reconstructed results are not superior to the one obtained by filter of size  $3 \times 3$ .

## 4. Experimental Results

In this section, eight different testing images are employed as shown in Fig. 4. The Eq. (3) is adopted for evaluating average PSNR, where the LMS-trained filter of size  $7 \times 7$  is involved in the performance evaluation.

First, we try to determine the best diffused weighting and the corresponding diffused area. Figure 5(a)-(d) shows the dot-diffused images processed by the four optimized class matrix with different diffused weighting of size. Among these, Fig. 5(a) has the maximum PSNR of 33.3 dB which associates to LMS

filter of size 3x3. The exact coefficient values are shown in Fig. 6, where the variable  $x$  denotes the current processing pixel. The average PSNR versus the class matrices derived from different diffused area are shown in Fig. 7. It is clear that the image quality decreases according to the increasing in diffused area, which is quite reasonable that the correlation decreases as distance increasing from the center. Hence, in this work the class matrix trained by LMS filter of size 3x3 as shown in Table II is employed for the proposed dot diffusion.

A series of experiments are conducted for comparison between Mese's and the proposed dot diffusion. In Mese's dot diffusion, the sole tone 16 is utilized for class matrix optimization. Conversely, in this work, eight nature images are employed for optimization. In Fig. 8, the whole grayscale ranging from 0 to 255 are involved for testing. It is clear that the proposed method is mostly superior to Mese's method. The average PSNR of the proposed method and Mese's method are 35.26 dB and 32.46 dB, respectively. Another comparison is conducted with ramp map as shown in Fig. 9. The result is complied with the former experiments as well, where the PSNR of the proposed method and the Mese's method are 35.1 dB and 32.4 dB, respectively.

Figure 9 shows the halftone results obtained by various halftoning methods, which include error diffusion by Floyd [5], Jarvis [6], Stucki [7], Ostromoukhov [8] and Shiau [11]; dot diffusion by Knuth [3] and Mese [4]; ordered dithering [1] with Classical-4 clustered-dot dithering and Bayer-5 dispersed-dot dithering; and DBS [13]. According to the experimental results, it is clear that the proposed dot diffusion has close image quality to error diffusion and far better than ordered dithering. Although the quality is still a bit lower than some error diffusion and DBS, the parallel processing nature is still an attractive advantage comparing to error diffusion or iteration-based DBS.

## 5. CONCLUSIONS

In this work, the parallel processing feature of dot diffusion is preserved, while the deficiency gap with the error diffusion is reduced. A new optimized class matrix is proposed based on the new diffused weighting. Four different diffused areas are tested as well and proved that the one of size 3x3 offers the best result. Another difference from the previous Mese's optimization approach is that the nature images are involved in the class matrix optimization, while Mese's approach solely adopts tone 16 as the training set. Apparently, the proposed dot-diffused results mostly have better quality in other tones. As demonstrated in the experiments, the quality of the proposed dot diffusion is close to error diffusion. Moreover, since the important parallel processing benefit is preserved in the proposed dot diffusion, it provides higher executing efficiency than DBS or error diffusion. Hence, the proposed dot diffusion has great contribution to practical printing industry or color quantization applications.

## References

- [1] R. Ulichney, Digital Halftoning. Cambridge, MA. MIT Press, 1987.
- [2] D. L. Lau and G. R. Arce, Modern Digital Halftoning. New York: Marcel Dekker, 2001.
- [3] D. E. Knuth, "Digital halftones by dot diffusion," ACM Trans. Graph., vol. 6, no. 4, Oct. 1987.
- [4] M. Mese and P. P. Vaidyanathan, "Optimized halftoning using dot diffusion and methods for inverse halftoning," IEEE Trans. Image Processing, vol. 9, pp. 691-709, Apr. 2000.
- [5] R. W. Floyd and L. Steinberg, "An adaptive algorithm for spatial gray scale," in proc. SID 75 Digest. Society for information Display, pp. 36-37, 1975.
- [6] J. F. Jarvis, C. N. Judice, and W. H. Ninke, "A survey of techniques for the display of continuous-tone pictures on bilevel displays," Comp. Graph. Image Proc., vol. 5, pp. 13-40, 1976.
- [7] P. Stucki, "MECCA-A multiple-error correcting computation

- algorithm for bilevel image hardcopy reproduction," Res. Rep. RZ1060, IBM Res. Lab., Zurich, Switzerland, 1981.
- [8] V. Ostromoukhov, "A simple and efficient error-diffusion algorithm," Computer Graphics (Proceedings of SIGGRAPH 2001), pp. 567-572, 2001.
- [9] L. Velho and J. M. Gomes, "Digital halftoning with space filling curves," Computer Graphics, 25(4): 81-90, July 1991.
- [10] K. T. Knox, "Introduction to digital halftones." In R. Eschbach, editor, Recent progress in digital halftoning, pp. 30-33, IS&T, 1994.
- [11] J. N. Shiau and Z. Fan, "A set of easily implementable coefficients in error diffusion with reduced worm artifacts," SPIE, 2658: 222-225, 1996.
- [12] R. Eschbach, "Reduction of artifacts in error diffusion by mean of input-dependent weights," JEI, 2(4): 352-358, 1993.
- [13] Q. Lin and J. P. Allebach, "Color FM screen design using DBS algorithm," Proc. SPIE, vol. 3300, pp. 353-361, 1998.
- [14] R. A. Ulichney, "Dithering with blue noise," Proc. IEEE, vol. 76, pp. 56-79, Jan. 1988.
- [15] J. Mannos and D. Sakrison, "The effects of a visual fidelity criterion on the encoding of images," IEEE Trans. Inform. Theory, vol. 20, pp. 526-536, 1974.
- [16] Z. Wang and A. C. Bovik, "A Universal Image quality Index," IEEE Signal Processing Letters, vol. 9, no. 3, pp. 81-84, Mar. 2002.
- [17] N. Damera-Venkata, T. D. Kite, W. S. Geisler, B. L. Evans, and A. C. Bovik, "Image Quality Assessment Based on a Degradation Model," IEEE Trans. on Image Processing, vol. 9, no. 4, pp. 636-650, Apr. 2000.

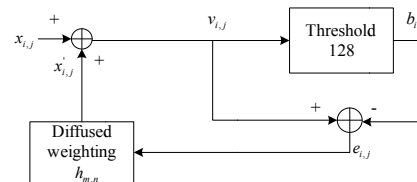


Fig. 1. Dot diffusion flow chart.

1	2	1
2	x	2
1	2	1

Fig. 2. Diffused weighting employed in Knuth's [3] and Mese's [4] dot diffusion.



Fig. 3. Eight training images of size 512x512.



Fig. 4. Eight testing images of size 128x128.



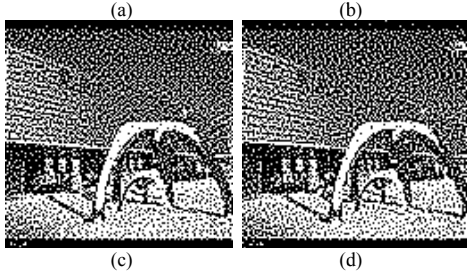


Fig. 5. Halftone images obtained with class matrix of different diffused areas. (a) Diffused weighting of size 3x3. (PSNR = 33.3 dB)(b) 5x5. (PSNR = 31.85 dB) (c) 7x7. (PSNR = 31.08 dB) (d) 9x9. (PSNR = 30.94 dB)

0.080009	0.126664	0.075175
0.121144	x	0.118328
0.079654	0.131194	0.081044

Fig. 6. LMS-trained diffused weighting of size 3x3.

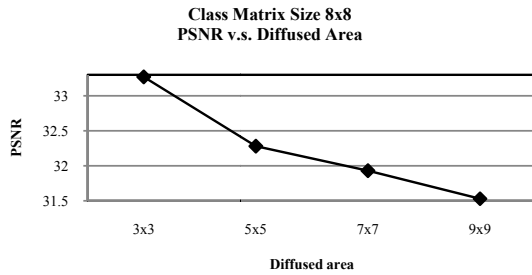


Fig. 7. Average PSNR using 8 testing images obtained by the proposed class matrices of size 8x8.

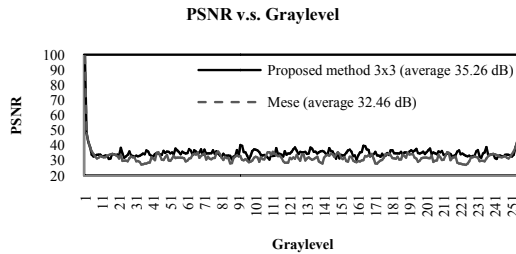


Fig. 8. PSNR v.s. Grayscale comparison between the proposed and Mese's dot diffusion.

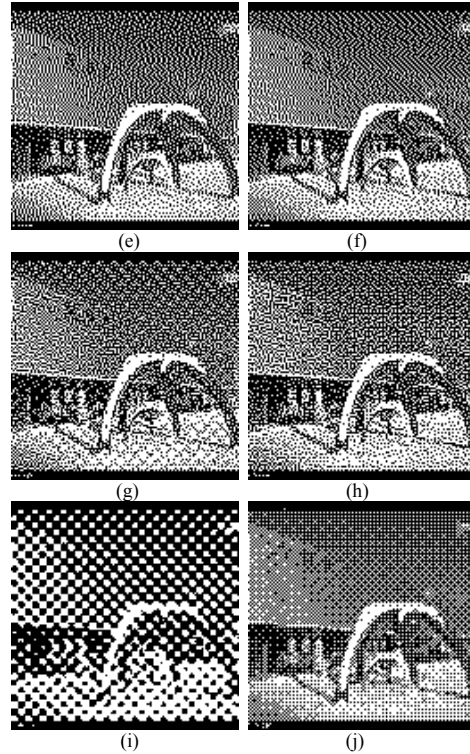
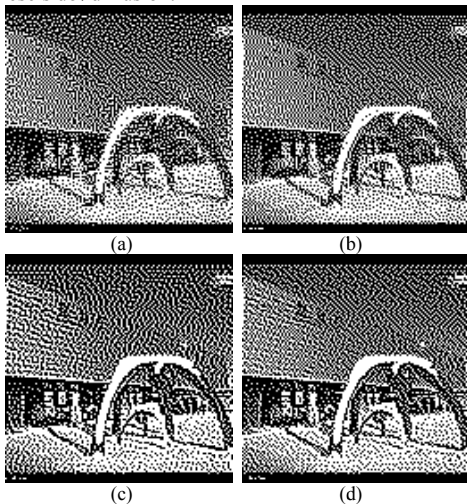


Fig. 9. Performance comparisons between various methods. (a) DBS [13]. (PSNR = 40.23 dB) (b) Floyd [5], (PSNR = 34.58 dB) (c) Jarvis [6], (PSNR = 28.41 dB) (d) Stucki [7], (PSNR = 29.05 dB) (e) Ostromoukhov [8], (PSNR = 35.33 dB) (f) Shiau [11], (PSNR = 34.67 dB) (g) Knuth [3]. (PSNR = 30.6 dB) (h) Mese [4]. (PSNR = 31.52 dB) (i) Classical-4 clustered-dot dithering. (PSNR = 18.91 dB) (j) Bayer-5 dispersed-dot dithering. (PSNR = 29.34 dB)

TABLE I. CLASS MATRICES OBTAINED BY KNUTH [3] AND MESE[4].

34	48	40	32	29	15	23	31
42	58	56	53	21	5	7	10
50	62	61	45	13	1	2	18
38	46	54	37	25	17	9	26
28	14	22	30	35	49	41	33
20	4	6	11	43	59	57	52
12	0	3	19	51	63	60	44
24	16	8	27	39	47	55	36
47	31	51	24	27	45	5	21
37	63	53	11	22	4	1	33
61	0	57	16	26	29	46	8
20	14	9	62	18	41	38	6
17	13	25	15	55	48	52	58
3	7	2	32	30	34	56	60
28	40	36	39	49	43	35	10
54	23	50	12	42	59	44	19

(a) Class matrix proposed by Knuth [3].

(b) Class matrix proposed by Mese [4].

TABLE II. CLASS MATRIX OBTAINED BY THE PROPOSED OPTIMIZATION PROCEDURE.

29	16	58	10	51	18	41	15
57	63	42	6	14	44	21	45
34	0	62	30	26	5	46	37
32	23	24	60	2	4	47	12
7	19	25	11	54	52	48	43
49	17	36	20	8	9	61	59
28	40	39	31	3	35	56	27
1	33	50	22	53	55	38	13

Diffused weighting of size 3x3.